

Growth dynamics of pulsed laser deposited Pt nanoparticles on highly oriented pyrolytic graphite substrates

R. Dolbec, E. Irissou, M. Chaker, D. Guay, F. Rosei, and M. A. El Khakani*

INRS-Énergie, Matériaux et Télécommunications, 1650 Boulevard Lionel-Boulet, C.P. 1020, Varennes, Québec, Canada J3X 1S2

(Received 13 July 2004; published 19 November 2004)

Platinum nanoparticles were grown by pulsed laser deposition (PLD) on highly oriented pyrolytic graphite substrates and characterized by scanning tunneling microscopy. Unexpectedly, as the nominal Pt thickness (t) is increased from 0.1 to 20 nm, the mean diameter (d_m) of the Pt nanoparticles follows the power law $d_m \propto t^{1/Z}$ with a dynamic exponent $Z=4.7 \pm 10\%$. This growth law is found to be valid for incident kinetic energy (K_E) of the ablated species involved in the growth process ranging from 4 to 130 eV/at. We also show that the shape of isolated Pt nanoparticles can be greatly influenced by K_E . Our results point out that PLD Pt nanoparticles nucleate and grow on the substrate rather than being formed in the ablation plume.

DOI: 10.1103/PhysRevB.70.201406

PACS number(s): 81.15.Fg, 61.46.+w, 68.37.Ef, 68.55.-a

Nanoparticles containing a few to thousands of atoms have recently been extensively investigated due to their unusual and surprising electrical, magnetic, optical, and chemical properties.¹⁻³ In the field of heterogeneous catalysis, spatially separated metallic nanoparticles on surfaces can exhibit pronounced size-dependent catalytic properties that differ considerably from those of single-crystal surfaces.^{4,5}

The pulsed laser deposition (PLD) technique is a very promising approach for the deposition of nanoparticles of various materials under a very wide range of growth conditions, thereby opening the prospects for the synthesis of novel nanostructured materials.⁶⁻¹¹ As an example, the PLD growth of silicon nanoparticles presenting a narrow size distribution has been studied for the development of new optoelectronic devices.¹⁰ For silicon nanoparticles, plasma spectroscopy-based experiments have shown that cluster nucleation and growth occurs in the ablation plume. However, in contrast with the conclusions of Ref. 10, this growth mode seems to apply only for some materials grown under specific deposition conditions. Indeed, nucleation and coalescence of nanoparticles on substrates have been reported for different laser-ablated metals, including Au/glass,¹¹ Fe/Cu(111),¹² Au/highly oriented pyrolytic graphite (HOPG),¹³ Fe/Mo(110),¹⁴ and Ag/Si.¹⁵ The model currently proposed for Si nanoparticles fails to describe the growth of these systems. There is thus a clear need for a model that describes the growth of PLD metal nanoparticles. Because platinum represents an ideal catalyst material in many applications,¹⁶ the particular case of the growth of Pt nanoparticles constitutes an especially interesting system, particularly so because the possibility of growing Pt nanoparticles with controlled dimensions in the nanometer range opens new avenues in the field of heterogeneous catalysis.^{3,4}

In this paper, we report a scanning tunneling microscopy (STM) investigation of the early stages of growth of Pt nanoparticles deposited by PLD onto HOPG substrates. The focus is put here on the growth dynamics of the Pt nanoparticles as a function of both the laser pulse number and the kinetic energy (K_E) of the ablated species (atoms, dimers, trimers, and clusters, etc.) in the ablation plume. In particular, the

analysis of our results in relation to a conceptual model points to a surprising analogy between Pt nanoparticle deposition by means of PLD over a wide range of incident kinetic energy and the apparently quite different (and much less energetic) molecular beam epitaxy (MBE) growth of metal nanoparticles.

Platinum nanoparticles were grown at room temperature by ablating a pure polycrystalline Pt target by means of a KrF excimer laser (wavelength=248 nm; pulse duration = 17 ns; repetition rate=20 Hz) in a high-vacuum deposition chamber (residual pressure $\sim 10^{-6}$ Torr). The laser beam was focused on the (5 cm \times 5 cm) Pt target (99.99% purity) at an incident angle of 45°. To perform deposition under reproducible ablation conditions, the target was continuously moved across the laser beam via a dual rotation and translation motion of the target holder. The on-target laser fluence was kept at about 4 J/cm². The substrates consisted of freshly cleaved HOPG samples mounted on a holder that is parallel to the target surface at a variable perpendicular target-to-substrate distance (D_{ts}). The nominal Pt thickness t was varied by increasing the number of laser pulses from 5 to 1000 under three distinct deposition conditions where D_{ts} and the helium background pressure were selected so as to obtain K_E values of 4, 45, and 130 eV/at.¹⁷ K_E values were deduced from time-of-flight (TOF) emission spectroscopy following the same procedure previously described¹¹ for the investigation of the expansion dynamics of gold ablated species. In the present study, the temporal evolution of the Pt plasma was obtained by recording the emission intensity of the Pt(I) neutral platinum line centered at 306.47 nm (lifetime of ~ 10 ns). The as-grown samples were then characterized *ex situ* using a commercial STM (NanoScope III, Digital Instruments) operated at room temperature in ambient air.

Typical STM images of the PLD Pt nanoparticles grown at $K_E=45$ eV/at. as a function of the number of laser pulses are presented in Fig. 1, together with their corresponding size distribution histograms. The STM images show that the Pt nanoparticles present a relatively round shape regardless of their size. No evidence of particle agglomeration or neck formation between nanoparticles was observed. As shown in

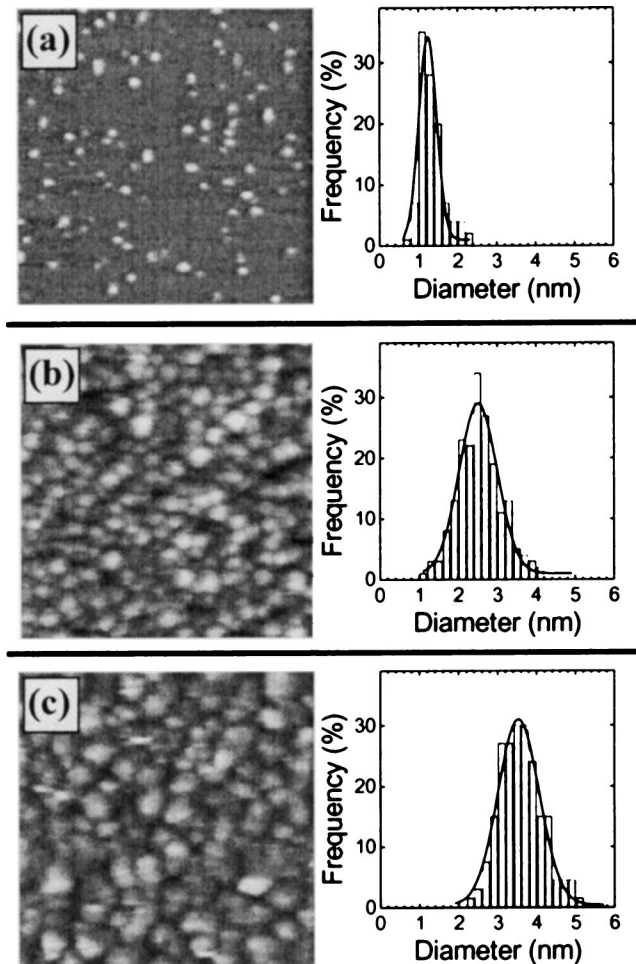


FIG. 1. Typical STM images and size distribution histograms for PLD Pt nanoparticles grown on HOPG under $K_E=45$ eV/at. at three selected nominal Pt thicknesses: (a) $t=0.1$ nm (five laser pulses), (b) $t=1$ nm (50 pulses), and (c) $t=10$ nm (500 pulses). The solid lines are Gaussian fits of the experimental data. The error on the mean diameter reported in the text corresponds to the FWHM of the Gaussian fit. The size of the STM images is 50×50 nm² (typical tip voltage and tunneling current were 1 V and 1 nA, respectively).

Fig. 1(a), the sample prepared with five laser pulses consists of spatially separated Pt nanoparticles randomly distributed on the HOPG surface. In this case, the mean diameter of the deposited nanoparticles (d_m) was found to be 1.25 ± 0.25 nm, while the equivalent Pt layer thickness (t) was estimated to be about 0.1 nm. As the number of laser pulses is increased from five [Fig. 1(a)] to 50 and to 500 [Figs. 1(b) and 1(c), respectively], the surface coverage has clearly increased, together with d_m , which increases from 2.5 ± 0.6 nm (for 50 pulses, $t \approx 1$ nm) to 3.6 ± 0.6 nm (for 500 pulses, $t \approx 10$ nm).¹⁸ It is also observed that under $K_E=45$ eV/at. a laser pulse number ≥ 50 (or $t \geq 1$ nm) is required to form a continuous film consisting of densely packed Pt nanoparticles (having a d_m of ~ 2.5 nm).

The dependence of d_m on the number of laser pulses for the three K_E conditions investigated here (4, 45, and 130 eV/at.) is presented in Fig. 2(a). In these three cases, d_m

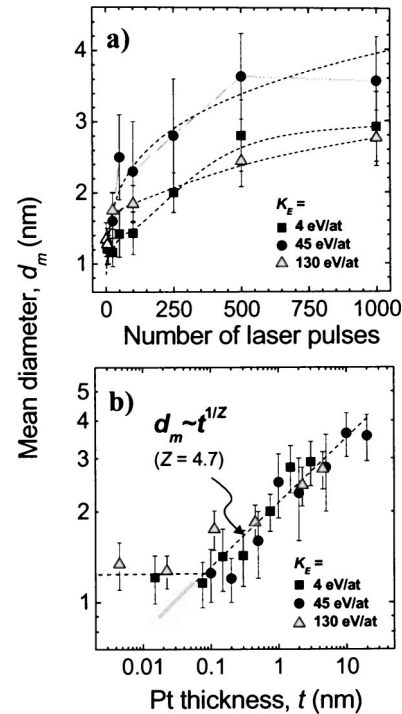


FIG. 2. Variation of d_m as a function of (a) the number of laser pulses, and (b) the nominal deposited Pt thickness, for the three K_E conditions investigated. For $t \geq 0.1$ nm, a growth law showing a dynamic exponent $Z=4.7 \pm 10\%$ has been evidenced.

is found to increase in a similar manner with the number of laser pulses. However, because of the higher deposition rate under the 45 eV/at. condition,¹⁷ in comparison to the two other K_E conditions, the films obtained under a given number of laser pulses are naturally thicker and consequently their constituting particles are slightly larger. This shows that the number of laser pulses is not necessarily the most appropriate parameter to compare the three K_E conditions investigated in this study. Instead, it was preferred to use the equivalent deposited Pt thickness¹⁹ as a common experimental parameter. Hence, the evaluation of t for each of the d_m values displayed in Fig. 2(a) has permitted us to plot d_m as a function of t as shown in Fig. 2(b), in a log-log plot form. Remarkably, all d_m values, regardless of the magnitude of K_E , are found to follow some sort of universal law in which two distinct growth regimes can be clearly distinguished. For $t < 0.1$ nm, the Pt nanoparticles have an average value of d_m of about 1.3 ± 0.3 nm [as those shown in Fig. 1(a)]. The fact that d_m remains somewhat constant with t could be ascribed to a nucleation regime, and suggests that energetic impinging species diffuse along the HOPG surface until they reach a thermodynamically stable nucleation site. Such an enhanced diffusion behavior is not surprising since the high mobility of the ablated species on the substrate is one of the specific features that distinguish PLD from other deposition methods.^{7,14} Moreover, motion of metal adatoms over typical distances in the 4–12 nm range has been reported for Au/HOPG grown by PLD,¹³ in agreement with the internanoparticle distance of 3–11 nm measured from Fig. 1(a). For the second growth regime ($t \geq 0.1$ nm), the Pt nanoparticles are now found to grow in size with t . Indeed, an unexpected

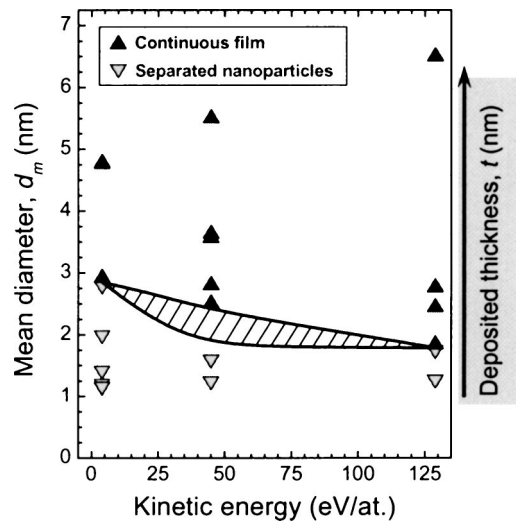


FIG. 3. All d_m values are reported as a function their respective growth condition. Open symbols (∇): spatially separated Pt nanoparticles. Filled symbols (\blacktriangle): Pt nanoparticles forming a continuous film. The hatched area illustrates the separation of the two growth domains and defines the limit size (d_{mT}) for the growth of spatially isolated nanoparticles for the three K_E conditions investigated here.

linear relation between $\log(d_m)$ and $\log(t)$ is obtained [Fig. 2(b)]. From a fit of the experimental data, we find a growth law of the type $d_m \propto t^{1/Z}$, with a dynamic growth exponent $Z = 4.7 \pm 10\%$. Surprisingly, this Z value is very comparable with those reported for different metals grown by a rather different method such as MBE.²⁰

Similar growth behaviors between MBE- and PLD-grown materials have also been reported for Fe islands grown onto Mo(110) substrates at room temperature. In this specific system, the Fe island density, as well as the mean island-to-island distance, were found to be the same, regardless of the deposition method (i.e., MBE or PLD).¹⁴ The authors explained this similarity by the fact that the high surface mobility (D) of laser-ablated species was compensated by the high instantaneous flux (F) of species impinging the substrate when deposition is performed at (or close to) room temperature, leading thereby to $(D/F)_{\text{PLD}} \approx (D/F)_{\text{MBE}}$. Such a relationship between D/F values could explain the similarity ($Z \sim 4$) we observed between MBE-grown materials and our results on PLD Pt nanoparticles.

The results presented in Fig. 2(b) showed that d_m is essentially independent of K_E for $t < 20$ nm, a result which is somewhat surprising at first. Considering that atoms deposited by MBE impinge the substrate with a typical K_E of about 0.1 eV/at. and that d_m follows the same growth law even when K_E is increased from 4 to 130 eV/at., it is legitimate to question how the excess energy of the Pt species would influence the growth kinetics of Pt nanoparticles deposited by PLD. Although there is no comprehensive answer yet, there is an effect due to K_E when the substrate coverage is only partial. Figure 3 reports all the d_m values presented in Fig. 2 as a function of K_E (error bars have been omitted for clarity). An open or filled symbol was used for each sample, according to whether our STM images revealed isolated nanoparticles such as in Fig. 1(a) (open symbol) or a continuous film

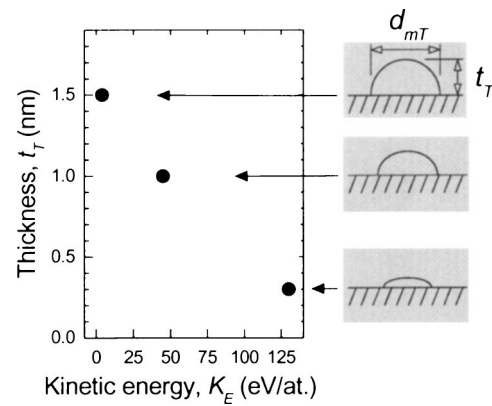


FIG. 4. Influence of K_E on the Pt thickness (t_T) measured at the limit size (d_{mT}) of spatially separated nanoparticles (hatched area in Fig. 3). Cross-sectional representations of corresponding Pt nanoparticles are displayed on the right-hand panel of the figure.

such as Figs. 1(b) and 1(c) (filled symbol). Therefore, as d_m increases with t for each K_E condition, a complete coverage of the HOPG surface by Pt nanoparticles is seen to occur at a given thickness, referred here to as a transition thickness (t_T). For each K_E condition, a corresponding transition mean diameter (d_{mT}) can be associated to this transition thickness. This d_{mT} value is located in the hatched area of Fig. 3 (which is intended only as a guide to the eye). By following the variation of this transitional d_{mT} value as a function of K_E , it is seen that d_{mT} noticeably decreases from about 3 to 2 nm when K_E is increased from 4 to 130 eV/at. This decrease of d_{mT} with increasing K_E can be interpreted by an increase of the density of surface defects created at the HOPG surface by impingement of the Pt ablated species.²⁵ Such an increase of surface defects, which act as nucleation sites for the diffusing Pt species, will naturally lead to a higher nucleation density with a concomitant reduction of d_m value.

Finally, by plotting t_T as a function of K_E (Fig. 4), we were able to gain insights on how the shape of the deposited nanoparticles is influenced by K_E . Indeed, Fig. 4 shows that at low K_E (4 eV/at.), spatially separated Pt nanoparticles reach their limit size at a t_T value of about 1.5 nm, a continuous film being formed for $t_T > 1.5$ nm. We emphasize that such t_T value is comparable to the radius of the nanoparticles ($d_m \approx 3$ nm while $t_T \approx 1.5$ nm), thus suggesting that hemispherical-shaped Pt nanoparticles are formed preferentially under low K_E deposition conditions. On the other hand, when K_E is high (130 eV/at.), Pt nanoparticles of ~ 2 nm diam form a continuous film when t is only of about 0.3 nm. In this case, the highly energetic impinging species are unlikely to land on the top of preformed Pt nanoparticles because of their high surface mobility. On the contrary, they are more likely to attach to new nucleation sites (whose density increases at the highest K_E , as discussed above) directly on the HOPG substrate or at the edges of existing Pt nanoparticles,²⁶ thereby leading to the growth of flattened nanoparticles, as was observed for other PLD grown systems like Fe/Cu(111) (Ref. 12) and Fe/Mo(110).¹⁴

In conclusion, by investigating the early stages of growth of Pt nanoparticles deposited by PLD on HOPG substrates, we were able to demonstrate that their size scales with the

deposited thickness, regardless of their K_E (K_E being in a range as wide as 4–130 eV/at.). In particular the $d_m \propto t^{1/2}$ growth law that typically applies to the MBE growth metal islands has also been shown to describe well the growth by PLD of Pt nanoparticles on HOPG substrates. In contrast to this growth law, which is independent of K_E , there is, however, a K_E effect on the size as well as on the transition thickness at which the transition from isolated particles to continuous film takes place. Indeed, the size of isolated Pt nanoparticle at this transition thickness was found to decrease somewhat from ~ 3 to 2 nm (Fig. 3) as K_E is increased from 4 to 130 eV/at. At this size limit, Pt nanoparticles grown at low K_E are hemispherical in shape, while those deposited at high K_E have a rather flattened shape (Fig. 4). These results demonstrate that, by properly adjusting not

only the magnitude of K_E but also the deposited thickness (i.e., the number of laser pulses), spatially separated nanoparticles with a range of nanostructured characteristics can be grown by PLD, allowing the investigation of their size-dependent properties with a fairly high degree of size control on the nanometer scale. It is left to future investigation to determine how or whether this might affect (for instance) the catalytic properties of the PLD Pt nanoparticles.

The authors would like to thank T.W. Johnston (INRS-EMT, Canada) and R. Rosei (Universita' di Trieste, Italy) for their valuable discussions and comments. This work was financially supported by the Natural Science and Engineering Research Council (NSERC) of Canada.

*Author to whom correspondence should be addressed. Electronic mail: elkhakan@inrs-emt.quebec.ca

¹W. Eberhardt, *Surf. Sci.* **500**, 242 (2002).

²K. H. Meiwes-Broer, *Metal Clusters at Surfaces: Structure, Quantum Properties, Physical Chemistry* (Springer-Verlag, Berlin, 2000).

³C. T. Campbell, *Surf. Sci. Rep.* **27**, 1 (1997).

⁴C. R. Henry, *Surf. Sci. Rep.* **31**, 231 (1998).

⁵M. Valden, X. Lai, and D. W. Goodman, *Science* **281**, 1647 (1998).

⁶D. H. Lowndes, D. B. Geohegan, A. A. Paretzky, D. Norton, and C. M. Rouleau, *Science* **273**, 898 (1996).

⁷D. B. Chrisey and G. K. Hubler, *Pulsed Laser Deposition of Thin Films* (Wiley, New York, 1994).

⁸A. M. Serventi, M. A. El Khakani, R. G. Saint-Jacques, and D. G. Rickerby, *J. Mater. Res.* **16**, 2336 (2001).

⁹N. Braidy, M. A. El Khakani, and G. A. Botton, *Chem. Phys. Lett.* **354**, 88 (2002).

¹⁰W. Marine, L. Patrone, B. Luk'yanchuk, and M. Sentis, *Appl. Surf. Sci.* **154–155**, 345 (2000), and references cited therein.

¹¹É. Irissou, B. Le Droff, M. Chaker, and D. Guay, *J. Appl. Phys.* **94**, 4796 (2003).

¹²P. Ohresser, J. Shen, J. Barthel, M. Zheng, Ch. V. Mohan, M. Klaua, and J. Kirschner, *Phys. Rev. B* **59**, 3696 (1999).

¹³A. V. Zenkevich, M. A. Pushkin, V. N. Tronin, V. I. Troyan, V. N. Nevolin, G. A. Maximov, D. O. Filatov, and E. Lægsgaard, *Phys. Rev. B* **65**, 073406 (2002).

¹⁴P. O. Jubert, O. Fruchart, and C. Meyer, *Surf. Sci.* **522**, 8 (2003).

¹⁵K. Seal, M. A. Nelson, Z. C. Ying, D. A. Genov, A. K. Sarychev, and V. M. Shalaev, *Phys. Rev. B* **67**, 035318 (2003).

¹⁶G. A. Somorjai, *Introduction to Surface Chemistry and Catalysis* (Wiley, New York, 1994).

¹⁷ K_E values were deduced from the TOF emission spectroscopy in the following deposition conditions: $D_{ts}=60$ mm, P(He) = 500 mTorr for $K_E=4$ eV/at., $D_{ts}=30$ mm, P(He)=500 mTorr for $K_E=45$ eV/at., and $D_{ts}=60$ mm under vacuum ($\sim 10^{-6}$ Torr) for $K_E=130$ eV/at..

¹⁸Pt thin films (having a thickness of about 10 nm) have also been characterized by x-ray diffraction (XRD). By using the Scherrer formula, the full width at half maximum of the XRD peaks yielded a mean crystallite size of about 3.8 nm. This value is in very good agreement with the d_m value of 3.6 ± 0.6 nm obtained from STM analyses, thereby confirming the discrete character of the Pt nanoparticles that form the continuous film.

¹⁹For each deposition condition, the nominal Pt thickness (t) is obtained by multiplying the number of laser pulses by the deposition rate (in nm/pulse) measured using a quartz crystal microbalance.

²⁰A theoretical work has shown that for MBE-grown metals Z is equal to 4 (Ref. 21). This agrees with different experimental studies. Indeed, $Z=4.3 \pm 10\%$ has been reported for Fe(001) grown by MBE on Mo(001) (Ref. 22); also $Z=4.55 \pm 10\%$ has been obtained for Fe/Fe(001) grown by MBE (Ref. 23). Similar results ($Z=4.2 \pm 10\%$) were also recently found in the case of Ag islands deposited by MBE on GaAs(001) (Ref. 24).

²¹M. Siegert and M. Plischke, *Phys. Rev. Lett.* **73**, 1517 (1994).

²²K. Thürmer, R. Koch, M. Weber, and K. H. Rieder, *Phys. Rev. Lett.* **75**, 1767 (1995).

²³Y. L. He, H. N. Yang, T. M. Lu, and G. C. Wang, *Phys. Rev. Lett.* **69**, 3770 (1992).

²⁴M. Fanfoni, E. Placidi, F. Arciprete, F. Patella, N. Motta, and A. Balzarotti, *Surf. Sci.* **445**, L17 (2000).

²⁵K. Bromann, C. Félix, H. Brune, W. Harbich, R. Monot, J. Buttet, and K. Kern, *Science* **274**, 956 (1996).

²⁶H. Brune, *Surf. Sci. Rep.* **31**, 121 (1998).